MECHANICAL PROPERTIES OF PRE-STRESSED FABRIC-REINFORCED CEMENTITIOUS MATRIX COMPOSITE (PFRCM)

Ernest Bernat-Maso[a*], Lluís Gil[a,b], Luis Mercedes[a] and Christian Escrig[a]

[a] Laboratory for the Technological Innovation of Structures and Materials (LITEM), Universitat Politècnica de Catalunya. C/ Colom 11, TR45. 08222 Terrassa

[b] Strength of Materials and Structural Engineering Department, Universitat Politècnica de Catalunya. C/ Colom 11, TR45. 08222 Terrassa

[*] Corresponding author. ernest.bernat@upc.edu

Abstract

Fabric Reinforced Cementitious Matrix (FRCM) is a composite strengthening material used to strengthen masonry and concrete structures in a passive way due to the requirement of crack activation. Prestressing fabric is proposed to overcome this limitation, to increase the cracking strength and to obtain a stiffer response. With this aim, over 200 tensile tests on FRCM specimens were performed to analyse the influence of prestressing fabrics. Other variables, like fixation system, testing speed, matrix material and fabric material, were also discussed. Evidences lead to conclude that prestressing fabric of FRCM is an effective way to increase its tensile cracking strength (over 30%) and tensile stiffness.

Keywords

FRCM, Pre-stressing, Experimental, Tensile test, Clevis

1. Introduction

Fabric Reinforced Cementitious Matrix (FRCM), also called Textile Reinforced Mortar (TRM) among other nomenclatures, is an inorganic matrix composite material initially developed with the aim of strengthening concrete and masonry building structures. Most of the authors (see[1]) reported the outstanding performance of this composite material at strengthening those structures, which generally increase their ultimate strength and ultimate deformation. However, the passive nature of FRCM makes it necessary to crack the mortar matrix in order to reach the full contribution of the textile reinforcement. In addition, this fact causes large deformations of strengthened structures, which might set the design limits into the serviceability field instead than into the ultimate strength field. Thus, it is though that assuring the collaborative contribution of fibre and matrix from the very beginning of the loading process is essential to avoid the early matrix cracking and to increase the stiffness of the strengthened structure.

In this line, the research presented herein wants to do a step forward on the improvement of this composite material by prestressing the fabric. It is a promising approach to fulfil the particular aim of guaranteeing the full mechanical collaboration between the two components of the FRCM and limiting the deformation of strengthened structures. Increasing the cracking load will contribute to enhance the durability of the strengthened element, whereas increasing the stiffness of FRCM will make it even more suitable for strengthening concrete structures because of improved mechanical compatibility. In addition, prestressing fabric would open the door to effectively precast thin FRCM elements with applications far beyond strengthening. Nevertheless, in-situ application of prestressed FRCM and the description of the required tools and methods are out of the scope of the current paper, which is focused to the experimental characterisation of this composite material in the case of prestressing the fabric.

47 Nevertheless, the idea of prestressing continuous fibres embedded into a cementitious matrix
48 is not completely new for author's knowledge. According to our records it was firstly proposed
49 in 2001 by Krüger et al. [2] who analysed the influence of prestressing carbon and aramid
50 rowings embedded into cementitious matrixes on the pull-out strength. They also analysed the
51 effect of coating fibres with epoxy resins to enhance bonding strength. A few years after, in
52 2007, Xu and Li [3] presented a study that analysed the influence of several parameters on the
53 fibre-matrix bond strength assessed using pull-out tests. One of these parameters was the
54 fibre prestressing. The same year, the research conducted by Peled [4] studied the influence of
55 low-tension (~7MPa) prestressed fabrics embedded into cement paste matrix by means of
56 flexural tests, pull-out tests and SEM observations combined with viscous-elastic tests of
57 fabrics to conclude that stiffer fabrics with reduced creeping are the ones which further
58 improve cracking performance of cement composites.

59 Recently, Gopinath et al. [5] studied the influence of stretching fabrics on the tensile response
60 of glass fibre FRCM specimens tested in clamped configuration. They concluded that
61 mechanical stretching (0.15% elongation) contributed to enhance first cracking load and led to
62 prevent sliding failure.

63 Thus, as far as we know, the tensile response of prestressed fabric reinforced cementitious
64 matrix (called PFRCM from now and on) has been little studied and most of the existing
65 researches are focused on analysing the bonding properties of prestressed fibres. Hence, the
66 main aim of this research is to analyse the performance of PFRCM specimens in order to
67 confirm the hypothesis that prestressing fibres would contribute to increase the cracking
68 strength and the elastic modulus prior to cracking. To do so, production procedures for PFRCM
69 specimens were defined and are reported with detail.

70 However, this novel research line required implementing tensile tests on FRCM specimens,
71 which were no really standardised. Despite the numerous research contributions carried out in

72 the recent years on FRCM and its use (see the review by Awani et al. [1]), there is no
73 agreement on the testing configuration yet. In this line, the research by de Felice et al. [6]
74 summarised several testing procedures implemented by different researchers. This situation
75 leads to difficulties on comparing results from different materials or different testing setups,
76 although the macroscopic response associated with different failure modes (early fibre
77 breaking, core filaments slippage and sleeve filaments slippage) has been previously discussed
78 (see [7])

79 A clear example is the diversity of specimens' sizes and shapes: 400x40x10 mm^3, 600x100x10
80 mm^3, 410x50x10 mm^3, 600x50x10 mm^3 and 400x32x6 mm^3 where respectively used by Carozzi
81 and Poggi [8], Larriñaga et al. [9], Arboleda et al. [10], De Santis and De Felice [11] and Escrig
82 [12]. Furthermore, some authors used bone-shape specimens (e.g. Raupach et al. [13])
83 increasing the diversity of specimen's geometric definition. A brief summary of used shapes
84 can be found in Hartig et al. [14], who reported the influence of the shape on the position of
85 the cracking area.

86 In the same line, a remarkable diversity of fixation systems of the specimens to the testing
87 machine have been proposed. Among them, direct clamping (see [8,12,15]) and Clevis fixation
88 (see [16]) are the most common ones. Other possibilities are soft clamping [17] or using hinged
89 steel flanges [13]. The influence of the fixation system has been widely studied (see [10,11])
90 concluding that clamped systems provide more stable response and greater load bearing
91 capacity whereas the matrix-fibre sliding process can only be assessed using tangential load
92 transmitting systems like Clevis one. This influence of the fixation systems on the failure mode
93 was also studied by Carozzi and Poggi [8].

94 Regarding the test execution, different testing deformation ratios have been used (see [8,10]),
95 mostly ranging from 0.1mm/min to 0.5mm/min but also changing the test speed depending on
96 the testing phase (before or after crack development). It is commonly recommended to

perform tests at 0.2mm/min according with AC434 [18] although little literature is available about the influence of this parameter. In addition, there is also an ongoing discussion about the methodology to measure the strains on specimens. On this topic, Escrig [12] proposed using strain gages but the cracking process affected the measurements. Larriñaga proposed using 210mm extensometer [19], which agrees with the proposals of Arboleda et al. [10] and Contamine et al. [20] of using the largest possible extensometers and placing up to four sensors if possible to take into account the likely bending effects during tensile testing.

Thus, a secondary aim of the current research was analysing the influence of testing speed and specimen fixation on the mechanical response of different FRCM systems (varying mortar and fabric beyond typical commercial prescribed combinations to wider research limits) in a comprehensive way to support the definition of the most suitable testing procedure for FRCM and PFRCM tensile characterisation.

2. Materials and methods

2.1. Mortar

Two different mortars were used to produce (P)FRCM specimens. The first one (*S*) is a structural reparation mortar (class R3 according with EN 1504-3 [21]) which includes short glass fibres and silica fume. The second one (*A*) is an auto-levelling mortar which includes fibres and organic additives.

The flexural strength and compressive strength of each mortar batch was experimentally determined according with EN 1015-11:2000 [22]. The particular and average values for these properties, along with their coefficient of variation, in brackets, are summarised in Table 1.

Mortar	***Batch***	***Flexural strength (MPa)***		***Compressive strength (MPa)***	
		Individual	*Average*	*Individual*	*Average*
S	S1	6.77	5.89 (0.16)	33.49	36.29 (0.16)
	S2	6.58		34.66	
	S3	5.25		44.81	
	S4	4.96		32.20	

A	A1	7.69	8.73 (0.21)	22.23	29.24 (0.25)
	A2	6.92		26.98	
	A3	11.01		39.50	
	A4	9.29		28.23	

Table 1. Mechanical properties of the mortars

2.2. Fabric

Two different fabrics were used to produce (P)FRCM specimens: carbon fibre (C) and basalt fibre (B). The properties of used meshes and constitutive fibres are summarised in Table 2. None of the fabrics was coated.

Tensile properties of a fabric are not equivalent to the tensile properties of a tow or the tensile properties of the corresponding fibre. Moreover, tensile strength depend on the testing setup, specimen geometry or fixation system. Thus, determining the representative ultimate tensile strength of fabrics when used in the particular prestressing configuration defined in this research (see the description of the setup in section 2.3 and Figure 1) was essential. In addition, this specific characterisation of fabrics must be done before prestressing them in order to prevent overpassing its maximum capacity during samples production. Possible local stress concentration effects (because of mechanical connection of the fabrics to the prestressing system), the influence of the fabrics' shape (1600 mm free length and 50 mm width) and possible slight misalignment of fabrics in the prestressing system (see Figure 1) might influence the tensile performance of fabrics reducing their apparent strength. Because of this, the prestressing system and the corresponding methodology (manual application of the load using tensors and controlled with two 10kN load cells up to failure within 3 minutes, see Figure 1) were used as testing machine to determine the representative tensile strength of this particular application of fabrics.

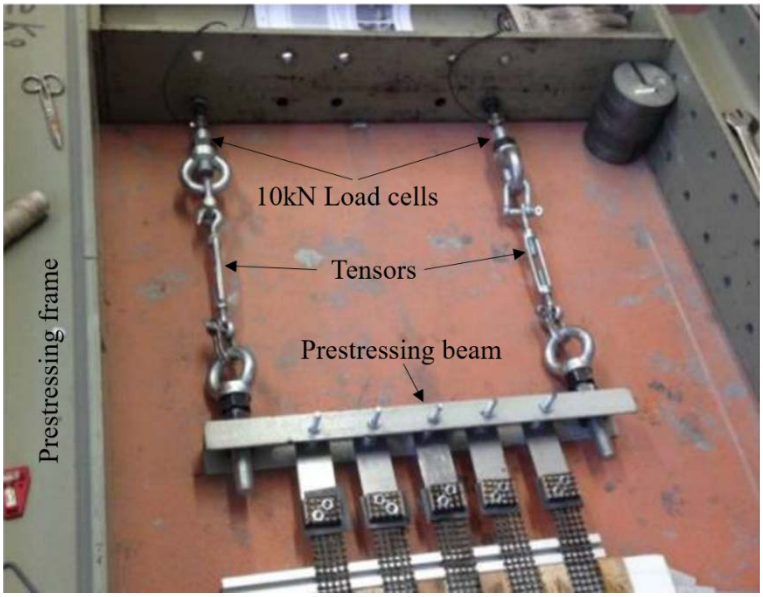

Figure 1. Fabrics connected to prestressing beam. Load cells to control prestressing load applied using tensors.

These previous tests resulted in a maximum load-bearing capacity of 1400N per prestressed basalt fibre fabric piece (50mm width) and 2200N per carbon one (same width). These values correspond to an equivalent maximum stress of 528MPa for basalt fabric and 936MPa for carbon fabric, proving that the equivalent maximum stress of a fabric is far lower than the fibre ultimate strength (summarised in Table 2. All values in this table expect for $f_{fab,u}$ and E_{tex} are reported in the corresponding data sheets). This fact was previously presented in other researches, like the one by Garmendia et al. [15] who reported a tensile strength of basalt textile of 505MPa in contrast with the corresponding fibre strength of 3080MPa. In fact, the observed failure mode, which was a progressive breaking of individual fibres, supports this idea because when testing a fabric not all fibres withstand the same load at an imposed displacement and the more loaded ones break causing an increase of the load of the rest of the fabrics that progressively break.

	Property	Units	Basalt (B)	Carbon (C)
Fibres	Ultimate tensile strength	$f_{fib,u}$ [MPa]	3080	4320
	Elastic modulus	E_{fib} [GPa]	95	240
	Ultimate strain	$\varepsilon_{fib,u}$ [%]	3.15	1.80
Fabric	Fibre orientation		Bidirectional	Bidirectional
	Equivalent thickness	t_{tex} [mm]	0.053	0.047
	Polymer coated rovings		No	No
	Distance between tows	d_{tows} [mm x mm]	15x15	10x10
	Elastic modulus[(1)]	E_{tex} [GPa]	63	113
	Ultimate tensile strength[(2)]	$f_{fab,u}$ [MPa]	528	936

[(1)] Values from previous research [12]

[(2)] Representative strength experimentally obtained for the particular prestressing system used in this research

Table 2. Properties of fibres and fabrics

2.3. Production method and specimens list

Two different production methods were implemented: one for the conventional FRCM specimens and another for the pre-stressed FRCM (PFRCM) specimens. In total 90 conventional specimens and 135 PFRCM specimens were produced. For each test type 15 specimens were produced to test 5 different loading ratios during tensile test with three repetitions per test. All 225 specimens had the same dimensions: 400mm x 50mm x 9mm. The maximum width (50mm) was limited by the width of the grips to be used in the clamped testing configuration, so it was littler than the minimum recommended one of 60mm (see [16]). The recommended ratio length/width ratio is respected resulting a total length of 400mm, which allowed the prescribed minimum central free length of 200mm. Finally, the thickness (9mm) fitted into the recommendations (>6mm) and corresponded to the typical thickness of wood strips used in the formwork.

The full relation of specimens is presented in Table 3. All samples are labelled with 3 letters, *ABC*, where *A* corresponds to the fixation system (C for clamped and H for hinged), *B* stands for the mortar type (S for reparation mortar and A for auto-levelling mortar) and *C* stands for the fabric type (C for carbon and B for basalt). In the case of pre-stressed samples two additional letters were include prior to the previous triplet resulting in a label like: *XY-ABC*, where *XY*

stand for the prestressing level (LP for low-prestressing level, MP for intermediate prestressing level and HP for high prestressing level).

Test type	*Mortar Batch*	*Fibre*	*Fixation*	*Prestressing level*	*Number of specimens*
CSC	S1	C	C	-	15
CSB	S1	B	C	-	15
HSC	S1	C	H	-	15
LP-HSC	S2	C	H	12.5%	15
HP-HSC	S3	C	H	35%	15
HSB	S1	B	H	-	15
LP-HSB	S2	B	H	12.5%	15
HP-HSB	S4	B	H	25%	15
HAC	A3	C	H	-	15
LP-HAC	A1	C	H	12.5%	15
MP-HAC	A3	C	H	25%	15
HP-HAC	A2	C	H	35%	15
HAB	A3	B	H	-	15
LP-HAB	A4	B	H	12.5%	15
HP_HAB	A3	B	H	25%	15

Table 3. List of produced specimens. Mortar batch according Table 1

In order to analyse the influence of the fixation system, specimens CSC and CSB were tested with clamped fixation in contraposition to specimens HSC and HSB whose endings were hinged using bonded steel plates (Clevis system). The rest of specimens were tested in hinged fixation configuration. Both mortars were combined with both fabrics. Conventional, low-prestressing (LP-) load PFRCM and high-prestressing (HP-) load PFRCM specimens were produced for each combination of mortar and fabric. Finally, an additional intermediate prestressing level was tested for specimens made of auto-levelling mortar and carbon fibre fabric (MP-HAC).

Conventional FRCM specimens were fabricated with the following procedure: (i) cutting mesh pieces to the corresponding dimensions (400mm x 50mm); (ii) mixing the mortar using a mechanical hand mixer and pouring a first layer of 4.5mm thickness into a mould of 9mm depth; (iii) placing the mesh on the fresh layer of mortar and softly press it; (iv) place the second layer of 4.5mm thickness of mortar to complete the volume; (v) vibrate the mould and regularise the top surface; and (vi) cure it for 14 days covered with plastic before unmoulding

and curing specimens at indoor environmental conditions (25°C±3°C and HR 45%±10%) for two additional weeks.

A novel procedure was implemented to produce prestressed PFRCM specimens:

a) Cutting long mesh pieces (1900mm x 50mm) to be able to hold them to the prestressing system.
b) Mechanical connection of the fabric. Holding the endings of fabric pieces by rolling them around a wood plate which was connected to a steel plate with bolts. Rubber plates were placed between the mesh and the bottom part of the wood piece and between the mesh and the connection steel plate to prevent fibre breaking. Similarly, wood is prefered for the auxiliary plate to prevent sharp edges and allow certain level of adaptability. In addition, tighten screws on the wood plate allowed a slight penetration of them assuring the conenction of the fabric. A mechanical connection was selected instead of a chemical one because of its applicability at a wider range of environmental conditions. See Figure 2.a.

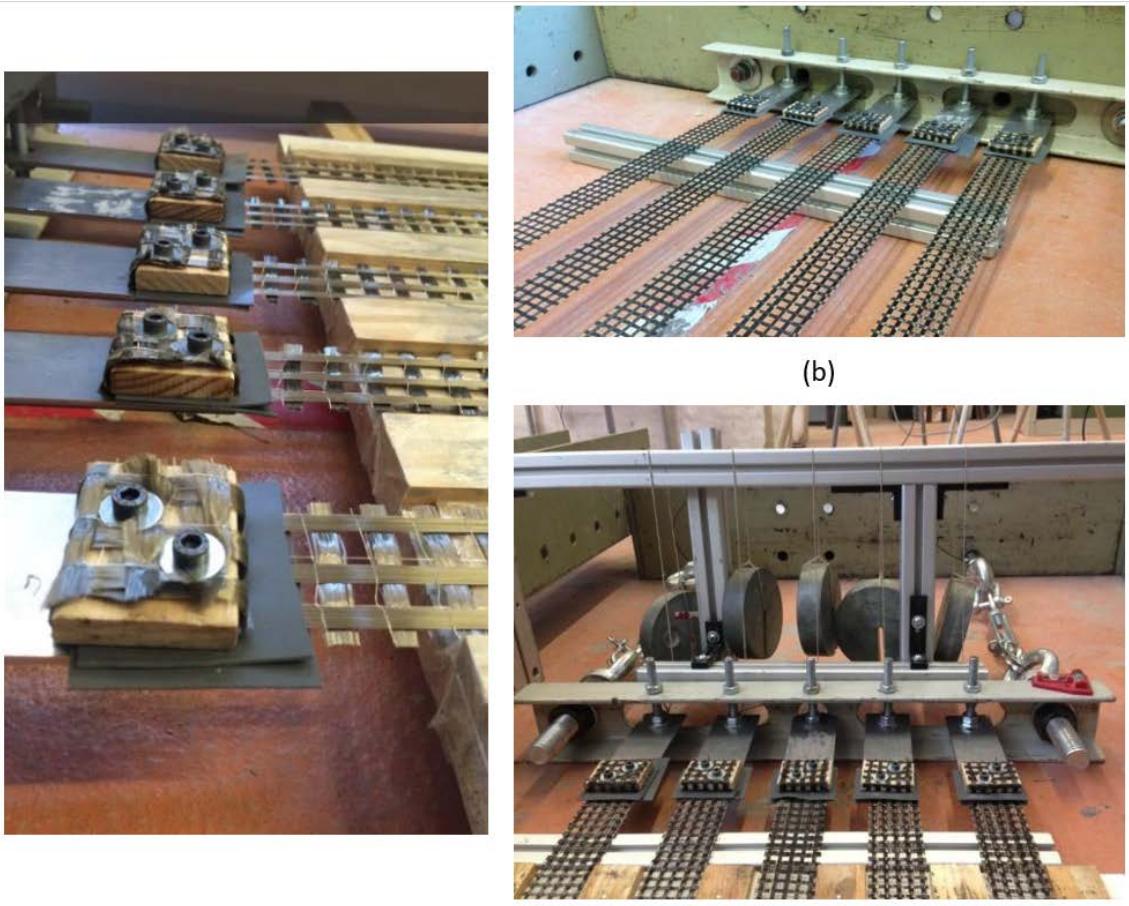

Figure 2. Fabric holding system (a), fixation to the prestressing frame (b) and preloading for fabric alignment (c)

c) Fixing one ending of the fibre mesh to the prestressing frame by holding the steel plate. See Figure 2.b.

d) Pulling horizontally from the opposite free ending to apply the same preloading to each fabric. This action assured a uniform load distribution among the five fabric lines when applying the pre-stressing load. This pulling action was undertook by hanging weights (2.5kg). See Figure 2.c and Figure 3.

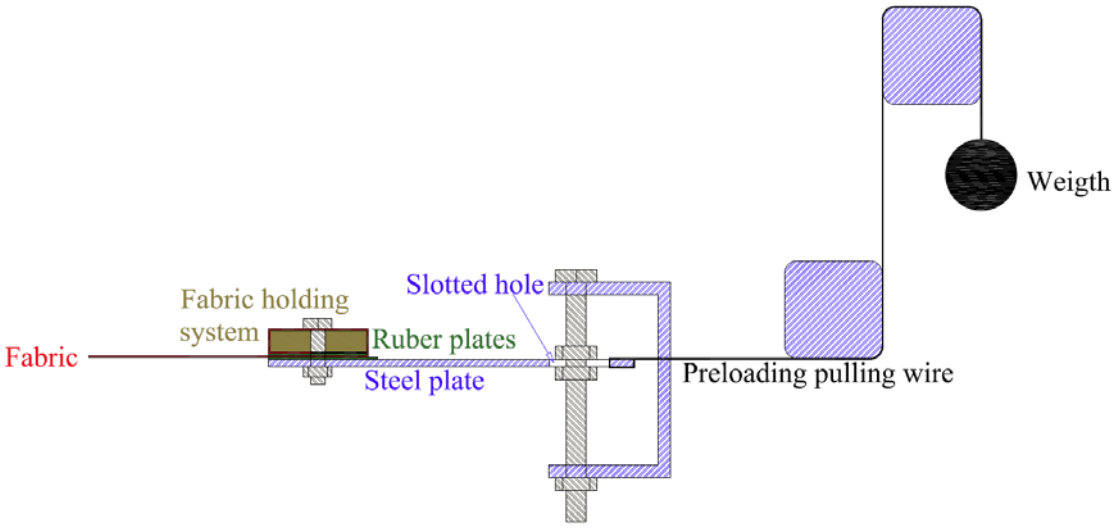

Figure 3. Sketch of the pulling system to apply preload on fabric strips

e) Repeat operations b-d for 5 identical fibre pieces.

f) Once the five fibre pieces were preloaded using the 2.5kg preload, their non-fixed endings were fixed to the moving prestressing beam (see Figure 1).

g) Prestressing fabrics to the desired level: 12.5%, 25% or 35% (see Table 3) of their maximum load-bearing capacity. The applied load was controlled using two load cells, which were connected to each extreme of the moving prestressing beam (see Figure 1).

h) Mixing the mortar using a mechanical hand mixer and pouring a first layer of 4.5mm thickness into the mould, which was designed to produce 5 PFRCM pieces of 1300mm length.

i) Placing the mould under the prestressed fabrics and level it up to reach the contact between the mortar layer and the prestressed fabric.

j) Casting the second layer of mortar to complete the 9mm thickness, vibrate the mould and cover it with plastic. See Figure 4. a.

k) Seven days after, the mould was released from the prestressing frame by cutting the fabrics. See Figure 4. b.

l) 14 days after casting, PFRCM pieces were unmoulded and cut to the desired length using a circular saw. See Figure 4. c.

m)

(a) (b) (c)

Figure 4. Casting the second layer of mortar once the mould was in the prestressing system (a), disconnecting the FRCM pieces from the prestressing system (b) and cutting specimens of PFRCM (c).

Once specimens were cured, their final preparation before testing depended on the testing fixation system. Clamped specimens (CSC and CSB) had the contact surfaces of their endings mechanically regularised by polishing. This same operation was undertaken for hinged specimens to assure the surface to be bonded to steel plates was perfect plain. Steel plates were bonded using bicomponent epoxy resin. To assure the correct alignment of connection steel plates a specific supporting system was used (see Figure 5). The bonded contact area between specimen and steel plates was 100mm x 50mm. The same preparation procedure was followed in previous successful researches (see [23]).

Figure 5. Bonding steel plates for hinged fixation testing

2.4. Testing method

Clamped specimens (CSC and CSB) were fixed between two rubber pieces to prevent direct clamp-specimen contact (see Figure 6.c), which might have introduced local stress concentrators. No relative sliding between specimen and clamp was observed due to the inclusion of the rubber piece. In this case (clamped specimens), strain was measured using a 25mm range 50mm initial distance extensometer, which was directly placed on the central position of clamped specimens (see Figure 6.a).

In contrast, hinged fixation was based on Clevis configuration but including an intermediate carabineer (see Figure 6.d) to allow all rotational movements. It was implemented for almost all tests reported herein. In this case, extensometer was placed on an auxiliary steel tool magnetically connected to the internal edges of the bonded steel plates. That allowed increasing the measuring reference length up to 200mm, being able to capture the average strain of the entire specimen (see Figure 6.b and [23]).

Tensile tests were carried out using an MTS Insight 10kN range electromechanic press. For each specimen configuration, 15 tests were carried out. Those included three repetitions for each one of the five different testing speeds: V1=0.2mm/min, V2=1mm/min, V3=5mm/min,

V4=25mm/min and V5=100mm/min. Force and strain measurements were automatically acquired at a ratio of 50Hz, which provided an average of 100 readings (2 seconds) for the fastest tests at V5 before cracking.

(a) (b)

(c) (d)

Figure 6. Extensometer positioning for clamped (a) and hinged (b) specimens. Clamped (c) and hinged (d) fixation systems.

3. Results

Analysed variables are the tensile cracking strength (f_{ft}), the effective elastic modulus prior to cracking (E_f*), the ultimate strength (f_{fu}) and the effective cracked modulus for the cracked specimens (E_f), if the specimens do not break immediately after cracking.

Cracking strength was calculated dividing the cracking load by the theoretical fibre area (specimen width = 50mm x equivalent thickness, t_{tex}). Ultimate strength was calculated dividing the ultimate load by the theoretical fibre area.

E_f* was calculated as the slope of the stress-strain curve before cracking load (see Figure 7), whereas E_f was calculated according with ACI 549.4R-13 [24].

Four failure modes were detected after analysing the broken specimens. The correspondence between failure modes and test typologies (materials, prestressing level and fixation system) is summarised in Table 4. Pictures of typical multiple cracking and one-crack failure are also included in Figure 7. It has to be noticed that there is no clear relationship between testing speed and failure mode.

Specimen type	***M-B***	***M-S***	***O-B***	***O-S***
CSC	V1-V5			
CSB	V3-V5		V1	V2
HSC	V1-V2	V3-V5		
LP-HSC		V1-V2		V3-V5
HP-HSC				V1-V5
HSB			V1-V3	V4-V5
LP-HSB				V1-V5
HP-HSB				V1-V5
HAC		V1-V5		
LP-HAC		V1-V5		
MP-HAC				V1-V5
HP-HAC		V1		V2-V5
HAB				V1-V5
LP-HAB				V1-V5
HP_HAB				V1-V5

Table 4. Main failure mode for each test type depending on the testing speed. M-B: Multiple cracking and fabric breaking; M-S: Multiple cracking and fabric sliding; O-B: One crack and fabric breaking; O-S: One crack and fabric sliding. Non-prestressed specimens are shadowed.

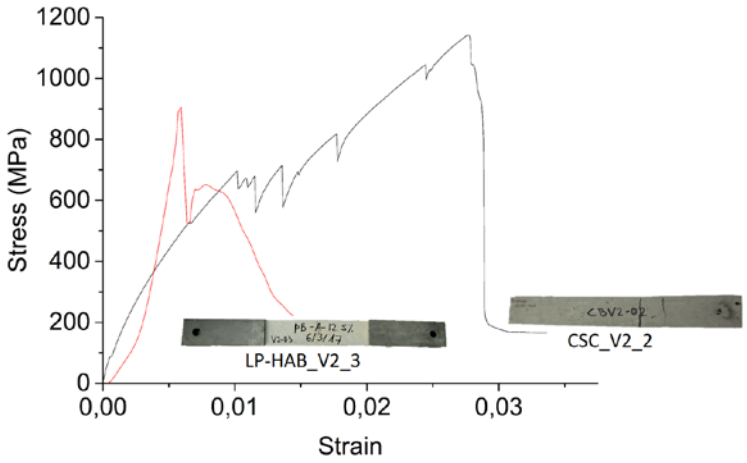

Figure 7. Typical stress-strain curves for multiple cracking (CSC_V2_2) and one crack and sliding (LP-HAB_V2_3)

Obtained results are presented in Figure 8 for strength values and in Figure 9 for elastic modulus and effective cracked modulus. It should be noticed that ultimate strength (f_{fu}) and effective cracked modulus (E_f) are missing for some specimens because those broke immediately after the first crack appeared (see Table 4 regarding failure modes) so the maximum load for these cases corresponds to the cracking one and no significant results were registered after cracking.

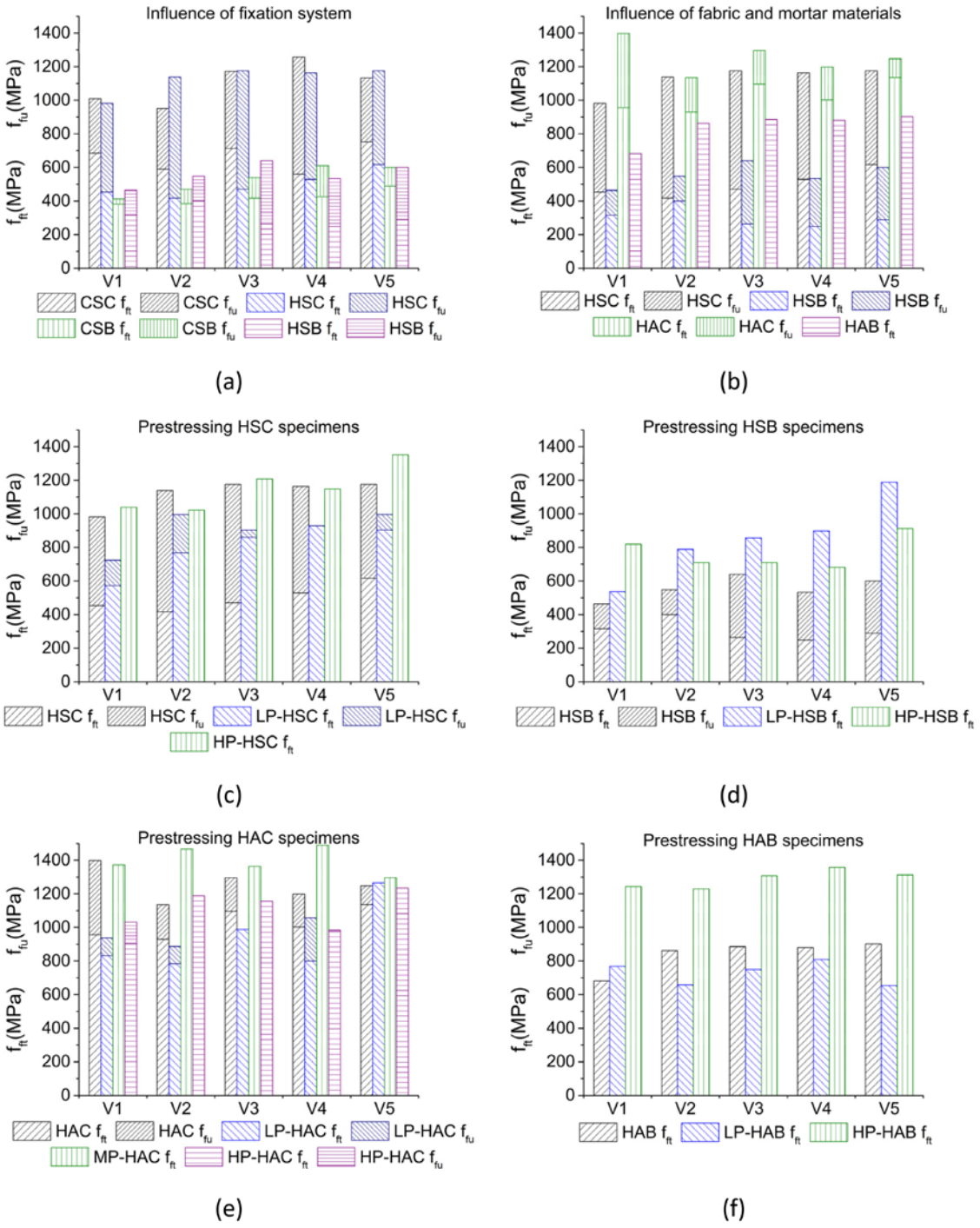

291

292 *Figure 8. Cracking (f_{ft}) and ultimate strength (f_{fu}) results for the five testing speed (V1-V5). Specimens labelling*
293 *according Table 3*

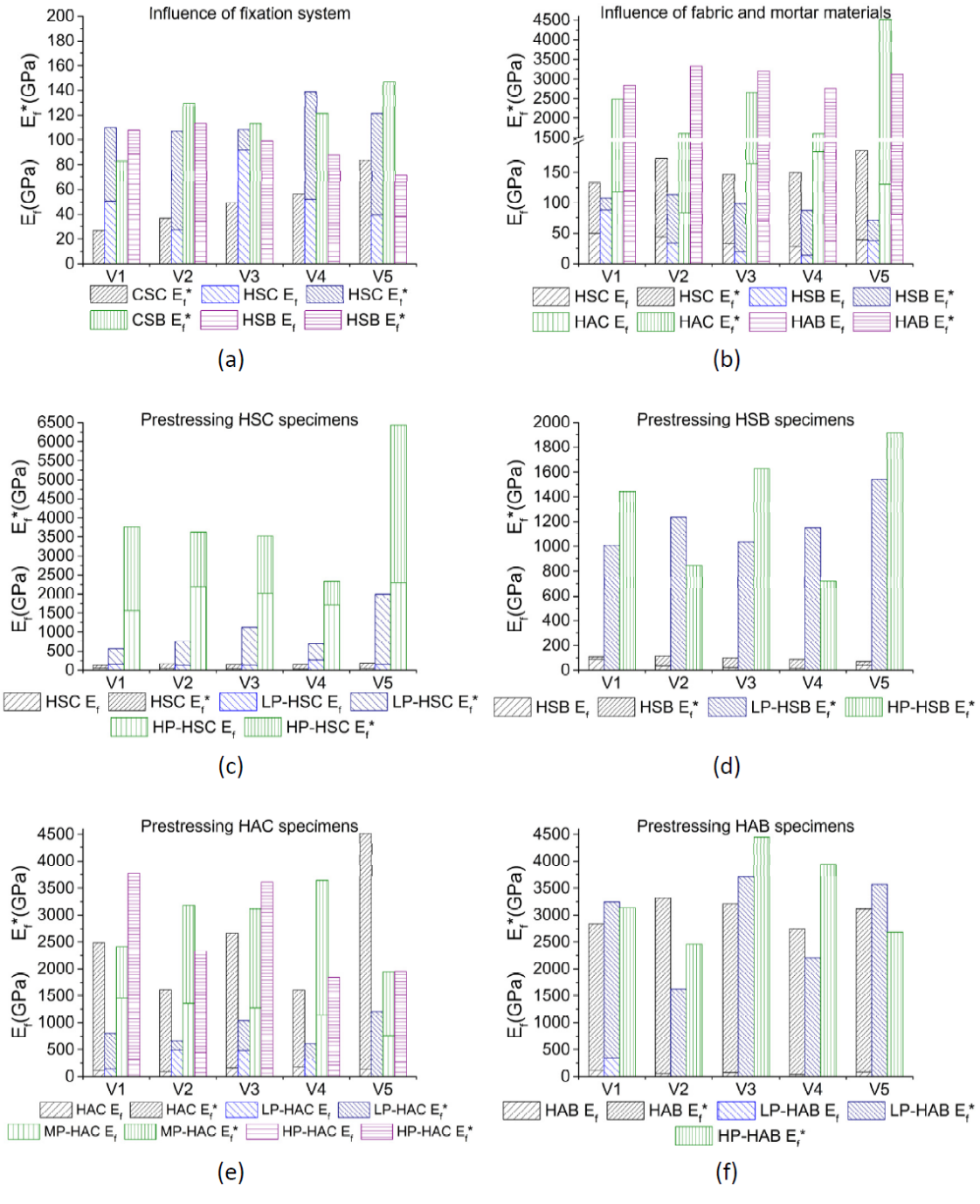

Figure 9. Elastic modulus prior to cracking (E_f) and effective cracked modulus (E_f) for the five testing speed (V1-V5). Specimens labelling according Table 3*

Regarding the variability of the results, Table 5 summarises the average coefficients of variation for every analysed property and testing speed. Extended results are included in Appendice A. Looking at these results, it is observed that coefficient of variation is around 16.5% for cracking tensile stress, 11.1% for ultimate tensile strength, 32.7% for elastic modulus prior to cracking and 30.2% for effective cracked modulus. This variability suggests that the analysis in terms of strengths (cracking and ultimate) will be more reliable than the analysis on deformability parameters.

Testing speed	f_{ft}	E_f*	f_{fu}	E_f
	CoV (%)	CoV (%)	CoV (%)	CoV (%)
V1	16.45	31.94	12.56	26.46
V2	13.65	32.72	8.51	28.93
V3	15.13	32.00	11.91	34.67
V4	18.40	34.79	11.30	34.91
V5	19.06	32.07	11.27	26.00

Table 5. Coefficient of variation of the different properties for every testing speed.

4. Discussion

4.1. Influence of the fixation system

First, it is noticed that fixation system influence on the developed failure mode (see Table 4). Hence, comparing CSC with HSC specimens and comparing CSB with HSB specimens it is observed that clamped system (CSC and CSB) allowed developing multiple cracking whereas specimens tested with hinged configuration (HSC and HSB) tended to develop only one crack. This fact is due to the normal compressive stress state introduced by clamps, which reduced fibre sliding possibilities. In consequence, it affected the fabric failure mode, which turns from breaking (clamped system) to sliding (hinged system) in general terms. Thus, the possibility of fabric sliding, which is theoretically associated with hinged fixation, prevents the development of multiple cracks. Hence, when the first crack opens the fibre slides and no more cracks are developed in most of the hinged cases. This phenomena is explained on the basis of the observations reported by Häußler-Combe and Hartig [7], who numerically proved that the sliding of the external filaments of a rowing respect the mortar matrix causes an increase of the crack separation.

Regarding the strength analysis (see Figure 8a), it is clear that cracking load for the tested hinged specimens is lower than for clamped ones. This evidence supports the previous idea that the normal compressive stress state introduced by clamps reduces partial fibre sliding possibilities, which turns into greater load requirements to reach the cracking strain of the composite material. In this line, previous researchers have obtained similar results: Arboleda

et al. [10] reported that the cracking load of clamped specimens was higher than the ones for Clevis supported comparable specimens. Similar results were obtained by Bianchi et al. [25] on tests on PBO-FRCM. However, other references point to the opposite. According with the tests conducted by de Santis and de Felice [11], the cracking stress of clamped specimens was lower than the cracking stress for hinged specimens. Hence, several variables are influencing the structural response up to the cracking load, being the mortar-matrix compatibility the prevalent one. A possible explanation to these different behaviours would be related with the fabric-matrix bonding. The contribution of the mortar confinement, which is associated to the clamping fixation, at preventing partial fabric sliding is not significant for those cases with an almost perfect bonding. In those cases, the stiffness of the gripping system can contribute to create parasitic bending moments or local stress concentrations (see [14]) in the transition area resulting in lower cracking strengths than the obtained using a hinged configuration. In contrast, those cases with partial interaction or not-so-perfect fabric-matrix bonding, which would be the case of non-commercial combinations like the ones used in the current research, can really benefit from the confinement provided by a clamped configuration that prevents partial fabric sliding and enhance pre-cracked performance respect to the tests using hinged configuration. Finally, in [11] it is also stated that the gripping method has little influence on the tests conducted on FRCM materials which show good adherence between fabric and matrix. Thus, fabric sliding possibility, which characterise the produced FRCM in the current research, may justify the described response prior to cracking and the influence of the fixation systems.

Regarding the influence of the gripping method on the ultimate strength, it was not really significant in the carried out tests since most of the specimens failed by fabric breaking at similar stress level. Thus, the ultimate strength is controlled by the textile as it was pointed out by de Santis and de Felice [11], who also noticed that the presence of multiple cracking (more common in the clamped specimens for the carried out tests) may cause local damage of the

fabric and a stress concentration effect that could bring to a slight reduction of the ultimate strength. This fact may explain the observed response of the tested specimens. Nevertheless, it has to be noticed that the influence of the gripping method on the ultimate strength reported in most of the previous researches point to the opposite: clamped configuration reached higher ultimate strength values than clevis (hinged) one because of the partial fabric sliding when coupons are tested under clevis configuration. This was the case of the experimental evidences provided by de Santis and de Felice [11], Bianchi et al. [25], Hartig et al. [14] and Arboleda et al. [10]. Hence, according with literature, the presented results regarding the influence of the gripping method on the ultimate strength may be explained because of three effects: (a) using non-commercial fabric-mortar combination may have caused little bonding between fabric and matrix even in the case of clamped gripping. (b) Misalignment and imperfections of the clamped specimens may have led to additional parasitic bending and partial breaking of fibres in the local contacts with cracks. (c) The presence of more cracks in the clamped coupons that translate to more points where local stresses on fabric may cause partial breaking of fibres. These three effects may have contributed to reduce the ultimate strength of the tested clamped specimens to the same range than the hinged (clevis) ones.

Observing the dependence of the elastic modulus (see Figure 9a) on the fixation system, it is noticed that clamped configuration reached higher non-cracked elastic modulus (E_f*) than hinged configuration in the case of basalt fabric specimens (CSB vs. HSB). This effect seems to point out that the adherence between used basalt fabrics and mortar matrixes was really affected by the fixation system. Moreover, this tendency was not observed for carbon specimens, which may have better adherence.

4.2. Influence of the mortar

In Figure 8b it is showed that increasing the tensile performance of the mortar causes a direct increase of the cracking strength of the composite material. Thus, cracking phenomena is mostly controlled by the mortar matrix for non-prestressed FRCM specimens. In addition, the ultimate strength of the specimens with carbon fabric also rises with the mortar tensile performance increase. However, HAB specimens failed just after cracking due to the relative lower strength of this fabric (1400N per specimen as presented before) in comparison with the high tensile strength of used auto-levelling mortar; whose tensile strength can be calculated from the flexural one to 4.86MPa[26]. This strength reached a total load-bearing capacity of 2200N per specimen. Thus, the basalt fabric was not able to withstand the applied load when the matrix cracked and the specimen failed.

In Figure 9b it is observed that elastic modulus prior to cracking (E_f*) significantly increase with the higher mortar performance, whereas effective cracked modulus is also increased but it is far less affected, showing that mortar influence is mostly noticeable during the pre-cracking stage.

Finally, it is observed (Table 4) that more specimens failed due to fabric sliding when auto-levelling mortar (A) was used instead of repair mortar (S). This fact can be related with fabric-mortar adherence. However, more research is necessary to confirm this particular statement.

4.3. Influence of the fabric

Influence of fabric type is analysed by comparing the response of HSC with HSB specimens and HAC with HAB specimens respectively. Regarding the cracking strength (see Figure 8b), it is clear that carbon fabric specimens reached higher stresses before cracking than basalt ones. This response is due to the higher elastic modulus of carbon fabrics, which restrained the strain in mortar requiring larger loads to crack it in comparison with basalt fabric reinforced mortar. According with de Santis and de Felice [11], this behaviour is possible because of a great mechanical performance of the used fabrics in comparison with the low performance of

402 the used mortars. In this situation, fabric influence on the first elastic phase may be
403 remarkable, whereas it has no influence in those cases that used high performance mortars
404 and relatively flexible fabrics. Finally, it has to be noticed that among the little references that
405 tested basalt and carbon fabric FRCM, the research conducted by de Felice [6] pointed out that
406 basalt-FRCM cracked at almost the same stress level than carbon-FRCM, indicating that mortar
407 was defining the response in the first elastic phase of their research. Hence, the tensile
408 response in the first elastic phase really depends on the particular combination of materials
409 considered.

410 The influence of the fabric type on the ultimate tensile strength is also noticeable: HSC
411 ultimate strength doubled the one for HSB, which was of the same order of magnitude than
412 the cracking stress of HSC specimens. This fact supports the idea that basalt fabrics
413 contribution is almost negligible after cracking. In relation with auto-levelling mortar
414 specimens (HAC vs. HAB), similar tendency was observed: HAC specimens increased the load
415 after cracking and their ultimate strength is in the range of the one for HSC, supporting the
416 idea that fabric controls the post-cracking response. In contrast, HAB specimens failed at the
417 cracking time due to the relative lower strength of that particular fabric.

418 The elastic modulus (Figure 9b) prior to cracking is higher for HSC specimens than for HSB
419 specimens, which was expected because of the higher value of the elastic modulus of carbon
420 fabric. However, the opposite response was recorded for specimens with auto-levelling
421 mortar. Thus, HAC specimens showed lower initial elastic modulus than HAB specimens for 4
422 of the 5 testing speeds analysed. This fact can be related with a better adherence between
423 auto-levelling mortar and basalt fabric than between the same mortar and carbon fabric. After
424 cracking, the effective cracked modulus of HSC and HSB are in the same order of magnitude
425 and no clear influence of the fabric type is observed. In contrast, HAC specimens showed

greater effective cracked modulus than HAB specimens, which clearly represents the fact that load-bearing capacity and stiffness of HAB specimens was drastically reduced after cracking.

Finally, fabric type influences on the failure mode (see Table 4). Carbon fabric specimens tend to show multiple cracking in far more proportion than basalt fabric specimens, for which the development of only one crack was dominant among the observed failure modes. This fact is related with basalt breaking or sliding immediately after the first crack appeared, which limited the possibility of developing new cracks.

4.4. Influence of the prestressing load

Analysing the influence of prestressing load needs to take into account the particular mortar batch used for each specimen series because of the significant influence of this parameter on the mechanical response. Hence, first analysed samples are those produced with the same mortar batch. Comparing HAC with MP-HAC (Figure 8e) and HAB with HP-HAB (Figure 8f) it is clear that prestressing fabric contributes to increase the cracking strength (f_{ft}) in a significant way (an average of 38% increase in the case of carbon fabric and 54% in the case of basalt fabric). It is justified because prestressing fabric causes a pre-compression stress state in the mortar matrix, which requires greater loads to be cracked. Regarding the ultimate tensile strength (f_{fu}), it has to be noticed that non-prestressed HAC specimens continued bearing higher loads after cracking, whereas MP-HAC failed at cracking load. In the case of HAB specimens, the maximum stress corresponded to the cracking one for all cases.

Elastic modulus of deformation before cracking (E_f*) of prestressed MP-HAC specimens (Figure 9e) is higher than non-prestressed HAC specimens for the three intermediate testing speeds and similar for the slower one. Similarly, elastic modulus of deformation before cracking (E_f*) of prestressed HP-HAB specimens (Figure 9f) is globally higher than the modulus for non-prestressed specimens (HAB) although the tendency is not so clear and even contradictory for testing speeds V2 and V5. In the case of the effective cracked modulus (E_f), it is clearly

451 increased when prestressing HAC specimens (comparing HAC and MP-HAC), whereas there is
452 no possible comparison in the case of HAB specimens whose typical failure mode included do
453 not withstand increasing loads after cracking.

454 Finally, regarding the failure mode (Table 4) it is observed that MP-HAC tend to fail with the
455 development of only one crack whereas non-prestressed contrast specimens (HAC) failed with
456 multiple cracking.

457 After analysing the possible direct comparison cases, the rest of tests are discussed taking into
458 account the diversity of mortar batches used. In the case of HSC specimens (see Figure 8c and
459 Figure 9c), increasing the pres-stressing load contributes to increase the cracking strength
460 although mortar flexural strength showed a minor reduction from S1 to S2 to S3 (see Table 1).
461 The ultimate tensile strength of HSC specimens was reduced with the application of little pre-
462 stressing level and no additional load was resisted after cracking in the case of high pre-
463 stressing level. Thus, when fibre breaking controls failure, prestressing fabric reduces the
464 ultimate strength of FRCM, although it can enhance the cracking strength so much to overpass
465 the non-prestressed ultimate tensile strength. Regarding the elastic modulus and effective
466 cracked modulus (see Figure 9c), these were increased with the pre-stressing load for prior and
467 after cracking stages, because fabric (stiffest material of the composite) contributed more to
468 the deformational response of FRCM composite. Nevertheless, the surprisingly high increase
469 for HP-HSC cases has to be analysed taking into account that S3 mortar showed over 30% of
470 increase in the compressive strength (see Table 1).

471 The same tendency of increasing cracking strength with pre-stressing level is observed for HSB
472 specimens (Figure 8d) except for the HP-HSB case, which used a clearly poorer mortar than the
473 other two cases of comparison. These cases also support the idea that pre-stressing FRCM
474 specimen tend to cause the failure at the cracking point although it happens at higher stresses
475 than the ultimate tensile strength of the comparison non-pre-stressed specimens. In the case

476 of HSB specimens (Figure 9d) the elastic modulus of the pre-cracking stage clearly increases
477 with the prestressing level, except for two particular test types involving HP-HSB specimens
478 produced with the poorer batch of the reparation mortar.

479 Analysing all HAC cases together (see Figure 8e and Figure 9e), the dependency of the tensile
480 cracking strength of FRCM on the mortar tensile strength (Table 1) is evident. A3 mortar had
481 higher flexural strength than A1 and this was higher than for A2 mortar batch. In consequence,
482 cracking strength of HAC specimens (A3 mortar) was higher than for LP-HAC specimens (A1
483 mortar) and the cracking strength increment form LP-HAC to HP-HAC (A2 mortar) cases was
484 littler than expected because HP-HAC specimens were produced with the mortar with lower
485 flexural strength. Regarding the ultimate tensile strength (f_{fu}), the efficacy of pre-stressing
486 fabric is also noticed because specimens produced with lower flexural strength mortar (HP-
487 HAC) reached higher maximum loads, although in those cases the maximum load was
488 registered at cracking time. In contrast, LP-HAC specimens bore additional load after cracking
489 in several cases. Similar tendency is observed for the elastic modulus before cracking and the
490 effective cracked modulus, which were higher for HP-HAC specimens than for LP-HAC
491 specimens although the former ones used a mortar with lower flexural strength.

492 In HAB analysis (see Figure 8f and Figure 9f), the same reasoning is possible. LP-HAB showed
493 lower cracking strength because LP-HAB specimens were produced with A4 mortar batch,
494 which had significant lower flexural strength than A3 batch used for HAB specimens. Regarding
495 the elastic modulus before cracking, no clear tendency was observed.

496 For all cases, it has been observed (Table 4) that increasing prestressing load tends to be
497 related with limiting multiple cracking in favour of one-crack development and it is also related
498 to increase sliding failure processes.

499 *4.5. Influence of the testing speed*

First, there is no relationship observed between the testing speed and the failure modes. In addition, it is neither possible to observe a clear dependency on the testing speed if comparing individual cases because of results variability (see Table 5) and little influence of this parameter.

The ratio of the mean value (3 repetitions) out of the average value for the testing speed V1 is calculated for testing speeds V2, V3, V4 and V5, for each specimen type and for each parameter (f_{ft}, f_{fu}, E_f* and E_f) to define a comparative dimensionless parameter, k. The idea is to assess if results for testing speeds V2-V5 are greater or smaller than the ones corresponding to the slowest tests. Results in comparison with reference case (V1=0.2mm/min) were k = 1.03, k = 1.17, k = 1.08 and k = 1.25 for testing speeds V2, V3, V4 and V5 respectively.

Thus, taking into account that V3 testing speed (5mm/min) reached a relative maximum of the comparison parameter (k) and that this speed can be maintained constant even for cases which show sliding processes in a reasonable total testing time, it is proposed to use 5mm/min as deformation ratio for FRCM tensile tests. Nevertheless, future additional testing campaigns are required to set or change this initial proposal, which is far faster than the typical testing rates used by other researchers, which tend to be in the range of 0.1mm/min to 0.5mm/min (see [8,27]).

5. Conclusions

An experimental campaign including 225 tensile tests on FRCM specimens has been conducted to analyse the influence of prestressing fabrics on the mechanical properties of FRCM. Additionally, the influence of fixation system, testing speed, mortar and fabric has also been studied.

Regarding pre-stressing technique, it can be concluded that:

- Prestressing fabric of FRCM contributes to increase the cracking strength over 30% and to increase the elastic modulus before cracking although more variability is observed on this parameter.
- Prestressing fabric of FRCM changes the failure mode preventing the development of multiple cracking and favouring fabric sliding.
- Prestressing fabric of FRCM causes a reduction of the tensile ultimate strength in those cases whose failure mode is controlled by the fibre tensile breaking. However, the cracking strength increase associated with prestressing process can overpass the non-prestressed ultimate tensile strength resulting in the situation that the cracking load turns to be the maximum one.
- Prestressing is especially effective in those cases whose failure mode is associated with fabric sliding.

Regarding testing configuration, it can be concluded that:

- Clamped fixation system tends to develop multiple cracking whereas hinged fixation system tends to be associated with only one crack development because of the more likely sliding of fabric.
- Clamped fixation tests resulted in higher values of cracking strength and non-cracked elastic modulus than hinged fixation tests. Ultimate tensile strength is not influenced by fixation system.
- Increasing the flexural strength of the mortar used as matrix of FRCM causes an increase of the cracking strength and the corresponding elastic modulus prior to cracking. Mortar influence is far more significant before cracking.
- Fabric properties control the mechanical response during the post-cracking stage if fabric tensile resistance is greater than matrix and adherence ones. Increasing fabric

547 stiffness contributes to increase FRCM stiffness before cracking if there is proper
548 adherence between matrix and fabric.
549 • It is proposed to use a testing speed of 5mm/min because it is associated with a
550 relative maximum of the FRCM performance and it allows using a constant
551 deformation rate even for the cases that slide.

552

553 **Appendice A**

554 Two tables summarising experimental results are included in this Appendice. For each test
555 type, the average value of the tensile cracking strength (f_{ft}), the effective elastic modulus prior
556 to cracking (E_f*), the ultimate strength (f_{fu}) and the effective cracked modulus for the cracked
557 specimens (E_f), if the specimens do not break immediately after cracking, are included. The
558 corresponding coefficients of variation are also reported.

Specimen type	*Test speed*	f_{ft}		E_f*		f_{fu}		E_f	
		(MPa)	*CoV(%)*	*(GPa)*	*CoV(%)*	*(MPa)*	*CoV(%)*	*(GPa)*	*CoV(%)*
CSC	*V1*	684	10,4	62	15,6	1009	20,0	---	---
	V2	590	10,1	74	0,8	951	17,9	---	---
	V3	713	6,6	110	20,7	1173	3,0	---	---
	V4	560	27,3	111	20,3	1256	7,3	---	---
	V5	752	10,2	129	9,1	1133	12,5	---	---
CSB	*V1*	382	12,4	110	52,0	413	10,2	---	---
	V2	385	22,1	107	13,7	470	12,1	---	---
	V3	417	7,5	108	15,2	539	7,2	---	---
	V4	426	10,6	139	11,9	611	14,7	---	---
	V5	490	12,1	122	41,2	599	14,5	---	---
HSC	*V1*	454	17,9	133	36,0	982	18,9	50	34,1
	V2	417	13,7	173	29,7	1138	3,7	44	34,9
	V3	470	26,1	147	41,7	1176	10,7	34	28,1
	V4	529	27,7	150	29,7	1163	10,7	28	35,4
	V5	617	14,5	186	4,4	1176	6,6	39	15,2
LP-HSC	*V1*	573	15,3	565	20,4	723	6,5	160	32,6
	V2	768	17,1	753	48,4	996	3,3	128	15,6
	V3	860	27,7	1125	57,0	903	11,0	133	52,5
	V4	929	11,1	689	59,6	929	6,1	271	53,3
	V5	904	13,8	1999	37,0	996	13,8	148	15,8
HP-HSC	*V1*	1040	5,8	3759	48,8	803	15,5	1556	24,7
	V2	1022	7,4	3626	96,0	968	2,7	2196	24,3
	V3	1208	10,1	3516	---	959	24,9	2018	31,0
	V4	1148	6,7	2330	0,2	1006	22,7	1713	10,0
	V5	1351	1,7	6441	24,7	1263	6,9	2300	11,6
HSB	*V1*	316	37,4	108	24,9	464	12,5	89	24,0
	V2	400	12,9	113	29,5	548	15,7	34	51,3
	V3	264	19,3	99	16,5	640	16,3	20	35,1
	V4	249	21,9	88	12,1	533	2,4	14	12,0
	V5	289	42,9	71	20,4	599	14,5	38	13,5
LP-HSB	*V1*	537	31,0	1009	4,0	---	---	---	---
	V2	788	17,7	1235	38,8	---	---	---	---
	V3	857	34,9	1038	21,7	---	---	---	---
	V4	898	11,7	1150	25,9	---	---	---	---
	V5	1187	20,6	1543	55,2	---	---	---	---

559 *Table A1. Results of the tensile tests on FRCM specimens (1/2)*

560

561

Specimen type	Test speed	fft		Ef*		ffu		Ef	
		(MPa)	CoV(%)	(GPa)	CoV(%)	(MPa)	CoV(%)	(GPa)	CoV(%)
HP-HSB	V1	819	22,9	1442	68,2	---	---	---	---
	V2	610	11,2	846	2,1	---	---	---	---
	V3	710	9,0	1629	76,3	---	---	---	---
	V4	682	42,9	718	75,4	---	---	---	---
	V5	913	31,2	1916	47,7	---	---	---	---
HAC	V1	955	10,5	2482	34,1	1398	12,3	119	42,1
	V2	929	10,7	1613	50,7	1135	18,6	84	12,3
	V3	1096	5,3	2661	30,8	1296	14,0	164	49,4
	V4	1002	2,0	1607	4,5	1198	11,7	183	44,8
	V5	1135	8,3	4519	47,8	1248	13,3	131	35,5
LP-HAC	V1	832	19,5	803	27,1	937	4,0	146	13,3
	V2	784	18,6	663	36,7	886	---	490	---
	V3	987	3,4	1039	25,0	932	14,7	481	64,7
	V4	800	1,8	608	7,3	1057	---	326	---
	V5	1265	---	1206	---	---	---	---	---
MP-HAC	V1	1373	6,7	2411	5,2	1061	8,5	1459	18,5
	V2	1466	1,3	3184	5,2	1069	5,4	1365	9,1
	V3	1364	8,3	3118	42,4	1146	3,6	1272	7,5
	V4	1490	14,4	3646	40,5	1157	5,6	1137	43,4
	V5	1297	4,2	1950	0,8	1216	2,7	759	16,2
HP-HAC	V1	902	15,9	3771	32,4	1032	7,7	316	22,1
	V2	1188	23,5	2325	27,1	1174	2,9	447	3,3
	V3	1155	7,8	3614	42,9	1143	5,6	160	15,9
	V4	976	40,4	1843	118,4	984	0,4	213	17,1
	V5	1234	8,4	1958	18,2	1186	10,7	268	71,0
HAB	V1	682	24,5	2836	40,8	547	9,9	120	26,8
	V2	862	8,7	3321	28,6	604	4,7	52	80,7
	V3	885	5,1	3208	23,7	581	9,9	70	27,8
	V4	880	9,1	2752	46,4	793	29,8	37	63,3
	V5	902	5,7	3115	3,8	653	6,3	81	29,3
LP-HAB	V1	769	13,1	3244	64,3	635	---	351	---
	V2	658	29,0	1625	56,0	---	---	---	---
	V3	750	40,8	3712	21,9	---	---	---	---
	V4	810	36,9	2205	35,9	---	---	---	---
	V5	654	71,3	3575	113,1	---	---	---	---
HP_HAB	V1	1243	3,8	3137	5,3	314	24,8	---	---
	V2	1229	0,9	2456	27,3	396	6,5	---	---
	V3	1308	15,0	4446	12,4	422	21,8	---	---
	V4	1357	11,4	3940	34,1	394	13,0	---	---
	V5	1312	21,8	2678	25,5	414	22,2	---	---

562 *Table A2. Results of the tensile tests on FRCM specimens (2/2)*

563

Acknowledgements

The support provided by undergraduate students Albert Rosell, Daniel de la Fuente, Joan Antoni Vila, Joan Margens, Miquel Pérez and Sergi Fernández to perform experimental tests is acknowledged. The contribution of SAHC master student Thomas Bose on developing the prestressing system is also acknowledged.

Funding

This research was partially funded as part of the MULTIMAS research project (BIA2015-63882-P) by the Spanish Government.

References

[1] O. Awani, T. El-Maaddawy, N. Ismail, Fabric-reinforced cementitious matrix: A promising strengthening technique for concrete structures, Constr. Build. Mater. 132 (2017) 94–111. doi:10.1016/j.conbuildmat.2016.11.125.

[2] M. Krüger, H.-W. Reinhardt, M. Fichtlscherer, Bond behaviour of textile reinforcement in reinforced and prestressed concrete, Otto-Graf-Journal. 12 (2001) 33–50.

[3] S. Xu, H. Li, Bond properties and experimental methods of textile reinforced concrete, J. Wuhan Univ. Technol. Mater. Sci. Ed. 22 (2007) 529–532. doi:10.1007/s11595-006-3529-9.

[4] A. Peled, Pre-tensioning of fabrics in cement-based composites, Cem. Concr. Res. 37 (2007) 805–813. doi:10.1016/j.cemconres.2007.02.010.

[5] S. Gopinath, R. Gettu, N.R. Iyer, Influence of prestressing the textile on the tensile behaviour of textile reinforced concrete, Mater. Struct. Constr. 51 (2018) 1–12. doi:10.1617/s11527-018-1194-z.

[6] G. de Felice, S. De Santis, L. Garmendia, B. Ghiassi, P. Larrinaga, P.B. Lourenço, D. V.

587 Oliveira, F. Paolacci, C.G. Papanicolaou, Mortar-based systems for externally bonded
588 strengthening of masonry, Mater. Struct. Constr. 47 (2014) 2021–2037.
589 doi:10.1617/s11527-014-0360-1.

590 [7] U. Häußler-Combe, J. Hartig, Bond and failure mechanisms of textile reinforced
591 concrete (TRC) under uniaxial tensile loading, Cem. Concr. Compos. 29 (2007) 279–289.
592 doi:10.1016/j.cemconcomp.2006.12.012.

593 [8] F.G. Carozzi, C. Poggi, Mechanical properties and debonding strength of Fabric
594 Reinforced Cementitious Matrix (FRCM) systems for masonry strengthening, Compos.
595 Part B Eng. 70 (2015) 215–230. doi:10.1016/j.compositesb.2014.10.056.

596 [9] P. Larrinaga, C. Chastre, J.T. San-José, L. Garmendia, Non-linear analytical model of
597 composites based on basalt textile reinforced mortar under uniaxial tension, Compos.
598 Part B Eng. 55 (2013) 518–527. doi:10.1016/j.compositesb.2013.06.043.

599 [10] D. Arboleda, F.G. Carozzi, A. Nanni, C. Poggi, Testing Procedures for the Uniaxial Tensile
600 Characterization of Fabric-Reinforced Cementitious Matrix Composites, J. Compos.
601 Constr. 20 (2016). doi:10.1061/(ASCE)CC.1943-5614.0000626.

602 [11] S. De Santis, G. De Felice, Tensile behaviour of mortar-based composites for externally
603 bonded reinforcement systems, Compos. Part B Eng. 68 (2015) 401–413.
604 doi:10.1016/j.compositesb.2014.09.011.

605 [12] C. Escrig, Estudio del comportamiento mecánico de vigas de hormigón armado
606 reforzadas a flexión y a cortante con materiales compuestos de matriz cementítica,
607 Universitat Politècnica de Catalunya, 2015.

608 [13] M. Raupach, J. Orlowsky, U. Dilthey, M. Schleser, Epoxy-Impregnated Textiles in
609 Concrete – Load Bearing Capacity and Durability, in: 1st Int. Conf. Text. Reinf. Concr.,
610 2006: pp. 77–88.

611 [14] J. Hartig, F. Jesse, K. Schicktanz, U. Häußler-Combe, Influence of experimental setups on
612 the apparent uniaxial tensile load-bearing capacity of Textile Reinforced Concrete
613 specimens, Mater. Struct. 45 (2012) 433–446. doi:10.1617/s11527-011-9775-0.

614 [15] L. Garmendia, P. Larrinaga, R. San-Mateos, J.T. San-José, Strengthening masonry vaults
615 with organic and inorganic composites: An experimental approach, Mater. Des. 85
616 (2015) 102–114. doi:10.1016/j.matdes.2015.06.150.

617 [16] RILEM Technical Committee 232-TDT (Wolfgang Brameshuber), W. Brameshuber, M.
618 Hinzen, A. Dubey, A. Peled, B. Mobasher, A. Bentur, C. Aldea, F. Silva, J. Hegger, T. Gries,
619 J. Wastiels, K. Malaga, C. Papanicolaou, L. Taerwe, M. Curbach, V. Mechtcherine, A.
620 Naaman, J. Orlowsky, P. Hamelin, H.W. Reinhardt, S. Shah, R. Toledo, T. Triantafillou, A.
621 Si Larbi, D. Garcia, L. Garmendia, S. Gopinath, F. Jesse, Recommendation of RILEM TC
622 232-TDT: test methods and design of textile reinforced concrete: Uniaxial tensile test:
623 test method to determine the load bearing behavior of tensile specimens made of
624 textile reinforced concrete, Mater. Struct. Constr. 49 (2016) 4923–4927.
625 doi:10.1617/s11527-016-0839-z.

626 [17] J. Hartig, F. Jesse, Evaluation of Experimental Setups for Determining the Tensile
627 Strength of Textile Reinforced Concrete, Int. RILEM Conf. Mater. Sci. – MATSCI, Aachen
628 2010 – Vol. I, ICTRC. I (2010) 117–127. http://demo.webdefy.com/rilem-new/wp-
629 content/uploads/2016/10/pro075-011.pdf.

630 [18] ICC Evaluation Serice Inc., AC434. Acceptance Criteria for Masonry and Concrete
631 Strengthening Using Fabric-reinforced Cementitious Matrix (FRCM) Composite Systems,
632 (2016).

633 [19] P. Larrinaga, Flexural strengthening of low grade concrete through the use of new
634 cement-based composite materials, Phd Thesis. E.T.S.I. de Bilbao. Universidad del País
635 Vasco, 2011.

636 [20] R. Contamine, A. Si Larbi, P. Hamelin, Contribution to direct tensile testing of textile
637 reinforced concrete (TRC) composites, Mater. Sci. Eng. A. 528 (2011) 8589–8598.
638 doi:10.1016/j.msea.2011.08.009.

639 [21] Committee AEN/CTN 83, UNE-EN 1504-3:2006. Products and systems for the protection
640 and repair of concrete structures - Definitions, requirements, quality control and
641 evaluation of conformity - Part 3: Structural and non-structural repair, (2006).

642 [22] Committee AEN/CTN 83, UNE-EN 1015-11:2000/A1:2007. Métodos de ensayo de los
643 morteros para albañilería. Parte 11: Determinación de la resistencia a flexión y a
644 compresión del mortero endurecido., (2007).

645 [23] L. Mercedes, L. Gil, E.B.-M.-C. and B. Materials, undefined 2018, Mechanical
646 performance of vegetal fabric reinforced cementitious matrix (FRCM) composites,
647 Elsevier. 175 (2018) 161–173. doi:10.1016/j.conbuildmat.2018.04.171.

648 [24] ACI Committee 549, ACI 549.4R-13 - Guide to design and construction of externally
649 bonded fabric-reinforced cementitious matrix (FRCM) systems for repair and
650 strengthening concrete and masonry structures, (2013).

651 [25] N.A. Bianchi G, Arboleda A, Carozzi FG, Poggi C, Fabric Reinforced Cementitious Matrix (
652 FRCM) Materials For Structural, (2013).

653 [26] Ministerio de Fomento. Comisión Permanente del Hormigón, EHE-08. Instrucción de
654 Hormigón Estructural, (2008).

655 [27] D. Arboleda, F.G. Carozzi, A. Nanni, C. Poggi, Testing Procedures for the Uniaxial Tensile
656 Characterization of Fabric-Reinforced Cementitious Matrix Composites, J. Compos.
657 Constr. 20 (2016) 04015063. doi:10.1061/(ASCE)CC.1943-5614.0000626.

658